Journal of Thermal Analysis and Calorimetry, Vol. 92 (2008) 2, 395–398

CALORIMETRIC AND THEORETICAL STUDIES ON THE SYSTEM OF {(*R*)-(+)-LIMONENE+(*S*)-(–)-LIMONENE}

M. Fujisawa[1]*, *S. Kido*[2] *and T. Kimura*[2]

[1]Department of Biotechnological Science, Kinki University, 930 Nishimitani, Kinokawa-City, Wakayama 649-6493, Japan
[2]Department of Chemistry, Kinki University, Kowakae, Higashi-osaka 577-8502, Japan

In order to reveal the origin of chiral discrimination, excess molar heat capacities (C_P^E) of ((*R*)-(+)-limonene+(*S*)-(–)-limonene) were determined by using a differential scanning calorimeter at temperatures between T=293.15 and 303.15 K. All C_P^E curves show S-shape. It was inferred that randomness appears in the (S)-(–)-limonene-rich region, and that non-randomness appears in the (*R*)-(+)-limonene-rich region. To clarify the differences in homochiral interactions and heterochiral interactions, molecular orbital calculations were carried out.

Keywords: *ab initio MO, chiral recognition, excess molar heat capacities, calorimetric and theoretical studies on the system of {(R)-(+)-limonene+(S)-(–)-limonene}, limonene*

Introduction

Elucidating the role of asymmetric intermolecular interactions due to the stereospecific structures of a molecule is important for understanding the mechanisms of reactions in chemistry and biochemistry. In particular, stereospecific interactions due to neighboring surfaces may play the leading role in, for examples, enzyme-substance reactions, antigen-antibody reactions, some kinds of mechanisms of the senses of smell and taste, etc. Takagi *et al.* [1, 2] discovered in 1966 that the small enthalpies of mixing of two enantiomers of some compounds are measurable by microcalorimetry. Later, other optical isomers were studied by Atik *et al.* [3, 4] also by microcalorimetry. Thereafter, the influences of stereospecific interactions and densities in the liquid state have been evaluated by others [5–11].

In order to understand the mechanisms of molecular discrimination and molecular behaviors of biological systems on the bases of intermolecular interactions and conformations of stereo-specific molecules, model compounds have been studied by measurements of heat capacities.

In our previous papers [12], the composition dependence of the excess isobaric molar heat capacity C_P^E at the temperatures 293.15, 298.15, 303.15 and 308.15 K were also determined for the system of (*R*)-(+)-α-pinene+(S)-(–)-α-pinene.

In this paper, the composition dependence of the excess isobaric molar heat capacity C_P^E at the temperatures 293.15, 298.15 and 303.15 K were also determined for the system of (*R*)-(+)-limonene+ (*S*)-(–)-limonene. To clarify the differences in homochiral interactions and heterochiral interactions, ab initio molecular orbital calculations were carried out. The correlation between the excess molar heat capacities and the interaction energies was discussed.

Experimental

(*R*)-(+)-limonene and (*S*)-(–)-limonene (ACROS. GR) were fractionally distilled over freshly activated molecular sieves 4A which had been evacuated at 453 K for 12 h under 10^{-2} to 10^{-3} Pa. Their chemical purities obtained from gas-vapour phase chromatography by using each 2 m column with FID on Yanagimoto G180FP are more than 99.9%. Water contents obtained by a coulometric Karl–Fischer's method on a Mitsubishi Moisture Meter, model CA-02 (Mitsubishi Chemical Ind.) are listed in Table 1. Densities of the samples measured by a vibrating-tube densimeter (Anton Paar D60) at 298.15±0.001 K are also listed in Table 2. The details of densitometric procedures were

Table 1 Purities of (*R*)-(+)-limonene and (*S*)-(–)-limonene at 298.15 K

Samples	Enantiopurity/ mol%	Water content/ mol%
(*R*)-(+)-limonene	99.9	0.030
(*S*)-(–)-limonene	93.3	0.042

---

* Author for correspondence: fujisawa@waka.kindai.ac.jp

1388–6150/$20.00

Akadémiai Kiadó, Budapest, Hungary
Springer, Dordrecht, The Netherlands

Table 2 Densities ρ of (*R*)-(+)-limonene and (*S*)-(–)-limonene

	ρ/g cm^{-3}		
	293.15 K	298.15 K	303.15 K
(*R*)-(+)-limonene	0.844415	0.842527	0.839979
(*S*)-(–)-limonene	0.844616	0.842728	0.840214

same as those described previously [13]. Enantiopurities of the samples were determined on a polarimeter (Horiba SEPA-200), and are listed in Table 1.

Calorimetric measurements were carried out using a VP-DSC differential scanning calorimeter (Microcal Corp. USA). Data were collected from 278 to 313 K at a heating rate of 0.0167 K s^{-1}. Molar heat capacities were calculated from the results for C_p/V using the densities of the mixtures, and of the pure components. The heat capacities were calibrated by using *c*-hexane and *n*-hexane.

Table 3 Heat capacities of (*R*)-(+)-limonene and (*S*)-(–)-limonene

T/K	C_p/J K^{-1} mol^{-1}	
	(*R*)-(+)-limonene	(*S*)-(–)-limonene
293.15	265.72	265.70
298.15	266.42	266.39
303.15	267.28	267.26

Results and discussion

Calorimetric

The isobaric molar heat capacities obtained for the pure enantiomers are listed in Table 3. The excess isobaric molar heat capacity for the binary system {*x*(*R*)-(+)-limonene+(1–*x*)(*S*)-(–)-limonene} was calculated by using the following equation

$$C_P^E = C_p - xC_{p,A} - (1-x)C_{p,B} \qquad (1)$$

where $C_{p,A}$ and $C_{p,B}$ are the molar heat capacities for (*R*)-(+)-limonene, for (*S*)-(–)-limonene, respectively, and C_p is the molar heat capacity of a mixture of {*x*((*R*)-(+)-limonene)+(1–*x*)(*S*)-(–)-limonene}, and *x* is the mole fraction of (*R*)-(+)-limonene. Composition dependence of excess molar heat capacity, at chosen temperature, is shown in Table 4 and Fig. 1., they are smoothed by the function:

$$C_P^E = \text{J K}^{-1}\text{ mol}^{-1} = x(1-x)\sum_{i=1}^{i=k} A_i\,(1-2x)^{i-1} \qquad (2)$$

where parameters A_i are given by a least-square method. The parameters are given in Table 5.

Excess molar heat capacities are negative for 0<*x*<0.45, and are positive for 0.45<*x*<1.0. Excess quantities of molar heat capacities are decreased slightly with increase of temperature. All curves show S-shape. It was inferred that randomness appears in the (*S*)-(-)-limonene-rich region, and that non-randomness appears in the (*R*)-(+)-limonene-rich region.

Table 4 Excess molar heat capacity C_P^E at constant pressure of {*x*(*R*)-(+)-limonene+(1–*x*)(*S*)-(–)-limonene}

x	C_P^E/J K^{-1} mol^{-1}		
	293.15 K	298.15 K	303.15 K
0.10251	–0.41	–0.38	–0.36
0.19980	–0.45	–0.40	–0.39
0.30152	–0.44	–0.41	–0.39
0.40082	–0.06	–0.06	–0.06
0.51452	0.13	0.13	0.12
0.62145	0.57	0.54	0.51
0.70684	0.64	0.62	0.58
0.79987	0.60	0.85	0.55
0.90454	0.45	0.42	0.40

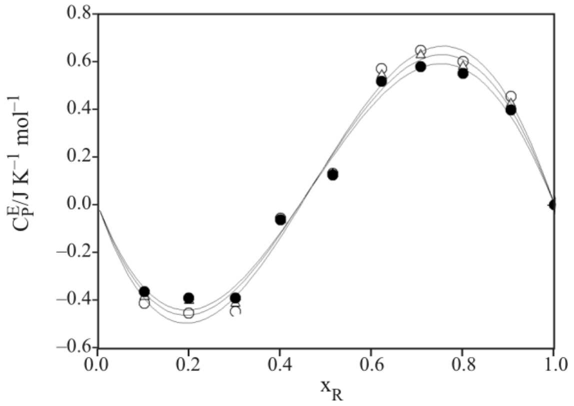

Fig. 1 Excess isobaric heat capacities C_P^E of {(*R*)-(+)-limonene+(*S*)-(–)-limonene},○ – *T*=293.15 K; △ – *T*=298.15 K; • – *T*=303.15 K

Table 5 Parameters of Eq. (2) for the excess molar heat capacity C_P^E at constant pressure of {*x*(*R*)-(+)-limonene+(1–*x*)(*S*)-(–)-limonene}

x	A_1	A_2	A_3	A_4	s_f
293.15 K	0.6874	–6.1316	–0.6088	0.6568	0.05
298.15 K	0.6602	–5.8651	–0.4222	0.8943	0.05
303.15 K	0.6582	–5.5098	–0.6406	0.7418	0.04

Theoretical

To clarify the differences in homochiral interactions and heterochiral interactions, ab initio molecular orbital calculations and DFT calculations were carried out. The Gaussian 03 program [14] was used for all molecular orbital method. The geometries of the (*R*)-(+)-limonene and (*S*)-(–)-limonene monomers were optimized at the B3LYP (Becke's three-parameter functional combined with Lee, Yang and Parr's correlation functional)/6-31G(d) level. The centers of gravity of the optimized enantiomers were arranged at the vertices of equilateral triangles with a 0.4 nm side length, and these structures were decided to the initial structure of conformational searches of the ternary systems. To decide the lowest energy conformer of the ternary system, conformation search was performed by COMFLEX6 program [15] with the MMFF94s force field. This program has the following feature; the lowest energy conformer does not depend on the initial structure that user input. The obtained three conformers with low energy were the initial structures of the molecular orbital calculations.

The geometries of the three ternary systems ((1) (*R*)+(*R*)+(*R*), (2) (*R*)+(*R*)+(*S*), (3) (*R*)+(*S*)+(*S*)) were optimized at the B3LYP/6-31G(d) level by the Gaussian 03 program. We selected the binary systems in the optimized ternary systems, and used the fixed structures of binary systems to decide the molecular interaction energies.

The molecular interaction energies of binary systems were calculated by using the following Eq. (3).

$$\Delta E(\text{int.}) = E(\text{binary system}) - \\ - E(\text{enantiomer 1}) - E(\text{enantiomer 2}) \qquad (3)$$

Electron correlation was accounted for by the MP2 (the second-order Moller–Plesset perturbation) and the B3LYP levels. All energy calculations by the molecular orbital method were done with the SCF=tight option. The total interaction energies were corrected by Basis Set Superposition Error (BSSE). The interaction energies of the binary systems were calculated at the MP2 and B3LYP levels using 6-31G(d) basis set, and were summarized in Tables 6 and 7.

In the (*R*)+(*R*)+(*S*) system, the homochiral interaction ((*R*)+(*R*)) is larger than the heterochiral interaction ((*R*)+(*S*)). This ternary system corresponds to (*R*)-(+)-limonene-rich region which is $C_\mathrm{P}^\mathrm{E}>0$. This situation indicates that the solution became non-random. The homochiral interaction ((*R*)+(*R*)) in the (*R*)+(*R*)+(*S*) system is larger than that in the (*R*)+(*R*)+(*R*) system. By mixing heterochiral molecule, it seems that the homochiral interaction became large. In the (*R*)+(*S*)+(*S*) system, the difference is small in the homochiral interaction ((*S*)+(*S*)) and the heterochiral interaction ((*R*)+(*S*)). This ternary system corresponds to (*S*)-(–)-limonene-rich region which is $C_\mathrm{P}^\mathrm{E}<0$. It seems that the S-shape curves arise from the variation of the molecular distribution in the chiral mixture with concentration composition. This is borne out by the discussion that uses Guggenheim's chemical lattice theory of solutions by Patterson *et al.* [16].

Table 6 Calculated interaction energies of the binary systems in the ternary systems at the MP2/6-31G(d) level

Ternary system	Binary sytem		
	(*R*)+(*R*)	(*R*)+(*S*)	(*S*)+(*S*)
(*R*)+(*R*)+(*R*)	-0.4_8	NA	NA
(*R*)+(*R*)+(*S*)	-2.2_8	-1.1_9	NA
(*R*)+(*S*)+(*S*)	NA	-1.1_4	-0.8_9

All data were given in kJ mol^{-1}

Table 7 Calculated interaction energies of the binary systems in the ternary systems at the B3LYP/6-31G(d) level

Ternary system	Binary sytem		
	(*R*)+(*R*)	(*R*)+(*S*)	(*S*)+(*S*)
(*R*)+(*R*)+(*R*)	-0.6_4	NA	NA
(*R*)+(*R*)+(*S*)	-2.9_5	-1.3_0	NA
(*R*)+(*S*)+(*S*)	NA	-0.7_6	-0.6_2

All data were given in kJ mol^{-1}

Acknowledgements

The authors wish to thank Mr. Yasushi Sakaguchi (Nihon SiberHegner K. K.) for assistance in the measurement of the excess molar heat capacities.

References

1 S. Takagi and M. Amaya, Abstracts of the Second Japanese Conference on Calorimetry and Thermal Analysis, Tokyo, 17–19 November 1966, p. 1.
2 S. Takagi, R. Fujishiro and M. Amaya, J. Chem. Soc. Chem. Commun., 10 (1968) 480.
3 Z. Atik, M. B. Ewing and M. L. McGlashan, J. Phys. Chem., 85 (1981) 3300.
4 Z. Atik, M. B. Ewing and M. L. McGlashan, J. Chem. Thermodyn., 15 (1983) 159.
5 J. P. Guetté, D. Boucherot and A. Horeau, Tetrahedron Lett., 29 (1973) 465.
6 L. Lepori, M. Mengheri and V. Mollica, J. Phys. Chem., 87 (1983) 1923.
7 A. Horeau and J.-P. Guetté, Tetrahedron, 30 (1974) 1923.
8 V. R. J. an den Oord, N. J. Breonese, L. J. F. Hermans and J. J. M. Beenakker, J. Chem. Phys., 85 (1986) 2193.
9 L. Lepori, M. Mengheri and V. Mollica, J. Phys. Chem., 98 (1994) 6862.
10 M. Shinitzky, A. Shvalb, A. C. Elitzur and Y. Mastai, J. Phys. Chem., B 111 (2007) 11004.

11 T. Kimura, M. A. Khan and T. Kamiyama, J. Therm. Anal. Cal., 85 (2006) 559.

12 M. Fujisawa, T. Matsushita and T. Kimura, J. Therm. Anal. Cal., 81 (2005) 137.

13 T. Kimura, Y. Usui, S. Nishimura and S. Takagi, J. Fac. Sci. Technol. Kinki Univ., 25 (1989) 109.

14 Gaussian 03, Revision D.01, M. J. Frisch, G. W. Trucks, H. B. Schlegel, G. E. Scuseria, M. A. Robb, J. R. Cheeseman, J. A. Montgomery, Jr., T. Vreven, K. N. Kudin, J. C. Burant, J. M. Millam, S. S. Iyengar, J. Tomasi, V. Barone, B. Mennucci, M. Cossi, G. Scalmani, N. Rega, G. A. Petersson, H. Nakatsuji, M. Hada, M. Ehara, K. Toyota, R. Fukuda, J. Hasegawa, M. Ishida, T. Nakajima, Y. Honda, O. Kitao, H. Nakai, M. Klene, X. Li, J. E. Knox, H. P. Hratchian, J. B. Cross, V. Bakken, C. Adamo, J. Jaramillo, R. Gomperts, R. E. Stratmann, O. Yazyev, A. J. Austin, R. Cammi, C. Pomelli, J. W. Ochterski, P. Y. Ayala, K. Morokuma, G. A. Voth, P. Salvador, J. J. Dannenberg, V. G. Zakrzewski, S. Dapprich, A. D. Daniels, M. C. Strain, O. Farkas, D. K. Malick, A. D. Rabuck, K. Raghavachari, J. B. Foresman, J. V. Ortiz, Q. Cui, A. G. Baboul, S. Clifford, J. Cioslowski, B. B. Stefanov, G. Liu, A. Liashenko, P. Piskorz, I. Komaromi, R. L. Martin, D. J. Fox, T. Keith, M. A. Al-Laham, C. Y. Peng, A. Nanayakkara, M. Challacombe, P. M. W. Gill, B. Johnson, W. Chen, M. W. Wong, C. Gonzalez and J. A. Pople, Gaussian, Inc., Wallingford CT 2004.

15 CONFLEX6, CONFLEX Corporation 2006.

16 M.-E. Saint-Victor and D. Patterson, Fluid Phase Equilib., 35 (1987) 237.

DOI: 10.1007/s10973-007-8958-y